Measurement of the low-wavenumber component within a turbulent wall pressure by an inverse problem of vibration

Damien Lecoq[a) and Charles Pézerat
Laboratoire d'Acoustique de l'Université du Maine (LAUM), Université du Maine, CNRS UMR 6613, Avenue Olivier Messiaen, 72085 Le Mans, Cedex 9, France

Fabien Chevillotte
Matelys-Research Lab, Bât. B, 7 rue des Maraîchers, 69120 Vaulx-en-Velin, France

Rémi Bessis
Institut Pprime, CNRS, Université de Poitiers-ENSMA, ENSIP, 6 rue Marcel Doré, Batiment B17, BP 633, 86022 Poitiers, France

An experimental validation is implemented for the measurement of a weak acoustic component within a turbulent wall pressure by an inverse problem of vibration. The turbulent flow is generated by a forward-facing step in a wind tunnel. In addition to the flow, an acoustic source with a low level excites the plate and plays the role of an additional acoustic component to be identified. The inverse methods called the force analysis technique and the corrected force analysis technique are used to compute the wall pressure fluctuations from the measurement of the plate vibration using an array of 13 accelerometers. The results show that contrary to the conventional techniques using pressure sensors, the inverse methods have a very good signal-to-noise ratio at the low wavenumbers. Indeed, the plate vibration is much more sensitive to the acoustic component than to the aerodynamic part. Moreover, this study shows that both methods can be used to isolate the weak acoustic part and identify its frequency spectrum. © 2016 Acoustical Society of America.
[http://dx.doi.org/10.1121/1.4962986]

I. INTRODUCTION

The improvement of the acoustic comfort in the transport industry is a major problem in engineering. In this context, the reduction of noise caused by turbulent flow in a vehicle is one of the important issues that need to be investigated. The motivation of this study is to better understand and predict the vibration generated by turbulent wall pressures responsible for noise inside a car. This work, therefore, deals with the bending of a plate, which is close to the windshield behavior, excited by a pressure field corresponding to a subsonic turbulent flow.

The wavenumber-frequency spectrum of the wall pressure due to a turbulent flow is typically represented in the (k_x, k_y) plane for a given angular frequency ω and is composed of two pats:[1] the aerodynamic component and the acoustic component [see Figs. 1(b)–1(d)]. In the case of an excitation due to a turbulent boundary layer, the energy of the aerodynamic component is located around the convective wavenumber k_{conv}, whereas that of the acoustic component is contained inside a circle whose radius is the acoustic wavenumber k_{ac} and has a very small amplitude.[2] These two components are very distinct in the (k_x, k_y) plane since $k_{conv} \approx 10 k_{ac}$ for automotive applications [see Fig. 1(a)]. That is

why they are called the low-wavenumber and the high-wavenumber components.

Unlike k_{conv} and k_{ac}, the flexural wavenumber k_f depends on the square root of the frequency [Fig. 1(a)]. k_f is closer to k_{ac} than k_{conv} for most frequencies. Indeed, in automotive glazing, the typical frequency for which $k_f = k_{conv}$ (the convective frequency f_{conv}) is a few tens of hertz, whereas those for which $k_f = k_{ac}$ (the coincidence frequency f_{ac}) is generally between 2 and 5 kHz. The vibration and the sound radiation of the plate are, therefore, strongly influenced by the acoustic component.

There are many semi-empirical models of wavenumber-frequency spectra for the turbulent boundary layer excitation.[3] The best known and most used in the case of a turbulent boundary layer are those of Corcos[4] and Chase.[5] In contrast to these two models, the latter model proposed by Chase[6] takes into account the compressibility of the fluid and, therefore, considers the acoustic component. However, the parameter used to adjust the level of these low wavenumbers is unknown and its experimental identification is difficult by using usual methods because the aerodynamic part is too high, and the signal-to-noise ratio (SNR) is too weak in the low wavenumbers.

Two kinds of experimental approaches can be found in the literature for the separation of these two components. The first is the use of an array of flush-mounted sensors.[7–11] In these cases, the authors used the spacing between the sensors and additional filters to separate the low and high
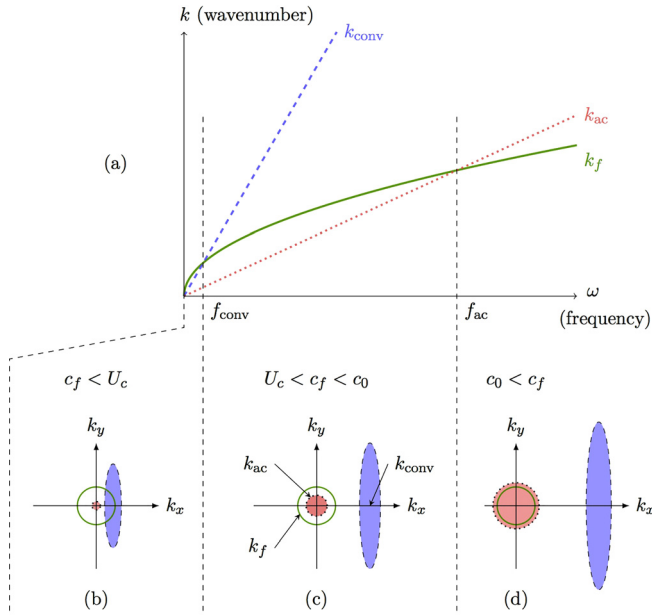
a)Electronic mail: lecoq.damien@gmail.com

FIG. 1. (Color online) (a) Evolution of the flexural (—), the convection (- - -), and the acoustic wavenumbers (···) as functions of frequency in a subsonic configuration and schemes of the frequency-wavenumber spectra (Refs. 1 and 3) of a turbulent flow excitation for (b) $f < f_{\mathrm{conv}}$, (c) $f_{\mathrm{conv}} < f < f_{\mathrm{ac}}$, and (d) $f_{\mathrm{ac}} < f$. The constants c_f, U_c, and c_0 are, respectively, the speeds of the flexion waves, the convections, and the acoustic waves.

wavenumbers. The major problem with this kind of device is that the dynamics of the sensors is insufficient to correctly measure the acoustic part. In addition, these methods are difficult to implement experimentally because they require the use of a large number of sensors mounted on plates that are specifically instrumented (with many holes, for example). The second approach is the use of vibration data. This is very useful to measure the low-wavenumber region since the plate is very sensitive to it. Martin and Leehey[12] used the modes of the plate to filter the turbulent wall pressure. This technique is rarely used because it is necessary to perfectly know the boundary conditions of the plate which are very difficult to assess.

In this study, we propose to use the force analysis technique (FAT),[13,14] which solves an inverse problem of vibration by providing the force distribution applied to a plate from vibration data. Unlike modal methods, this technique is local and there is no need to know the boundary conditions. A first study based on numerical simulations[14] reveals that FAT is able to measure an acoustic component in a turbulent boundary layer. This present work is the experimental validation where the corrected force analysis technique (CFAT)[15] is used to identify and isolate the low wavenumber part in a single point of a plate excited by a detached flow.

For this experimental study, the turbulences are created by a forward-facing step. For validation purpose, an acoustic component is generated by an additional source that is a loudspeaker whose level is set below the one of the turbulent wall pressure.

A brief overview of FAT and CFAT techniques are given in Sec. II. In addition, a new method is proposed to evaluate the spectral content in the wavenumber domain of the identified pressure by the comparison between the

frequency spectra obtained by FAT and CFAT. The experimental procedure, where a remote probe is also introduced in order to compare the results obtained with the inverse method, is then described in Sec. III. The reference spectra of the aerodynamic and the acoustic sources are also shown. In Sec. IV, the vibration spectra of the plate excited by the different sources are first analyzed. The frequency spectra of the pressures identified by FAT and CFAT are then compared to those measured by the remote probe when the source is only the acoustic component and when the excitation is the flow with the additional acoustic part.

II. THE FORCE ANALYSIS TECHNIQUE (FAT) AND ITS CORRECTED VERSION (CFAT)

FAT solves an inverse problem by injecting the measured displacement field into the plate equation discretized by a finite difference scheme. Through this approximation, the pressure p at the point (i, j) can be estimated from 13 displacement measurements around this point in the (x, y) plane of the plate:

$$p_{i,j}^{\mathrm{FAT}} = D(\delta_\Delta^{4x} + \delta_\Delta^{4y} + 2\delta_\Delta^{2x2y}) - \rho h \omega^2 w_{i,j}, \qquad (1)$$

with ω the pulsation, w the displacement, $D = Eh^3 / [12(1 - \nu'^2)]$ the rigidity, where E, h, ν', and ρ are, respectively, the Young's modulus, the thickness, the Poisson's ratio and the mass density of the plate. The approximation of the spatial derivatives of the displacement w by the 13-point finite difference scheme is computed through the terms δ_Δ^{4x}, δ_Δ^{4y}, and δ_Δ^{2x2y}. These expressions are given by Pézerat and Guyader.[13]

This inverse problem indirectly implies a very strong amplification of the high wavenumbers of the displacement field whereas the vibration is generally very weak in the wavenumbers far from k_f, the natural wavenumber of the plate

$$k_f = \sqrt[4]{\frac{\rho h}{D} \omega^2}. \qquad (2)$$

For this reason and since the input data of the method comes from vibration measurements, FAT essentially amplifies noise in these high wavenumbers. It is, therefore, necessary to apply a regularization to avoid this which is usually done by a low-pass wavenumber filtering requiring more measured points.

Recently, Leclère and Pézerat[15] showed that due to the discretization of the motion equation, the discrete finite differences used by FAT acts as a low-pass filter of the excitation in the wavenumber domain whose cutoff is close to the flexural wavenumber k_f. Their idea is to regularize the inverse problem by controlling this existing filtering that removes the high wavenumbers of the identified pressure contaminated by the measurement noise. To improve this filtering and avoid particular amplification of the error around the flexural wavenumber, they propose the CFAT which consists in changing the formulation of FAT in Eq. (1) by adding two corrective terms μ and ν,

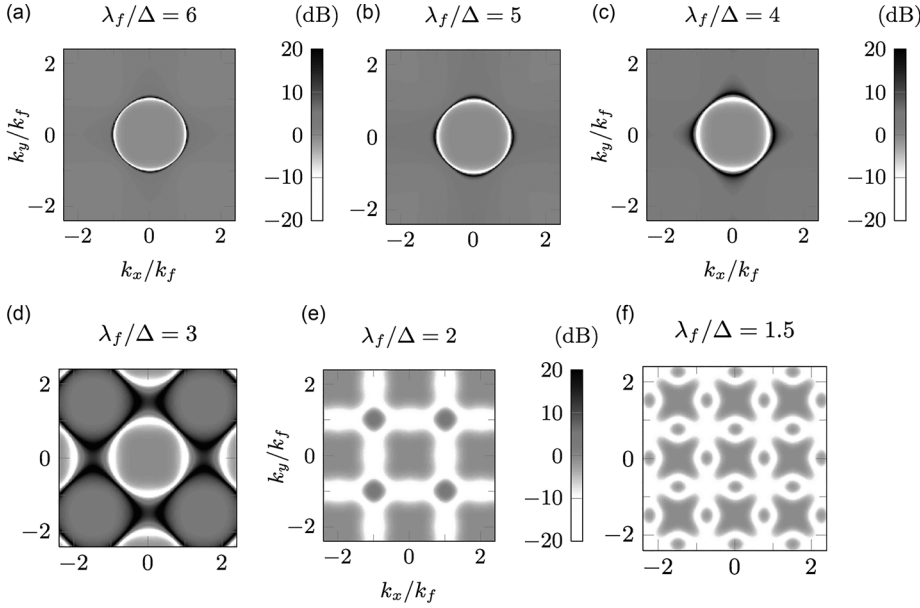J. Acoust. Soc. Am. **140** (3), September 2016

Lecoq *et al.* 1975

FIG. 2. Wavenumber responses $H(k_x, k_y, \omega)$ between p^{CFAT} and p^{FAT} for different values of λ_f/Δ, the number of points per wavelength.

$$p_{i,j}^{\text{CFAT}} = D(\mu^4 \delta_\Delta^{4x} + \mu^4 \delta_\Delta^{4y} + 2\nu^4 \delta_\Delta^{2x2y}) - \rho h \omega^2 w_{i,j}, \quad (3)$$

whose expressions are given by the authors:[15]

$$\mu^4 = \frac{\Delta^4 k_f^4}{4\left[1 - \cos(k_f \Delta)\right]^2}, \quad (4)$$

$$\nu^4 = \frac{\Delta^4 k_f^4}{8\left[1 - \cos\left(\frac{k_f \Delta}{\sqrt{2}}\right)\right]^2} - \mu^4. \quad (5)$$

The natural regularization provided by FAT and CFAT is valid in a certain frequency band for a given discretization Δ. Indeed, when the frequency increases, side lobes appear in the filter for wavenumbers above k_f, and when the frequency is too low, the filter is not sufficiently selective and does not remove the high wavenumbers contaminated by noise.[15] The domain of validity of these methods is empirically defined for frequencies such as $2 < (\lambda_f/\Delta) < 4$, where $\lambda_f = 2\pi/k_f$ is the natural wavelength.

In this study, FAT and CFAT are used to identify the pressure at one point from the measurement of the displacement in 13 points. Figure 2 shows the wavenumber responses $H(k_x, k_y, \omega)$ between these two methods for different number of points per wavelength calculated from the analytical expressions[15] of the spatial Fourier transforms $P^{\text{FAT}}(k_x, k_y, \omega)$ and $P^{\text{CFAT}}(k_x, k_y, \omega)$ of Eqs. (1) and (3):

$$H(k_x, k_y, \omega) = \frac{p^{\text{CFAT}}(k_x, k_y, \omega)}{p^{\text{FAT}}(k_x, k_y, \omega)}. \quad (6)$$

As expected, the methods are similar below k_f and very different around k_f because of the correction provided by CFAT. The idea is to use these wavenumber responses to extract information on the wavenumber spectrum of the pressure measured at a single point: if FAT and CFAT give the same results, the identified information is necessarily below k_f.

III. DESCRIPTION OF THE EXPERIMENTAL PROCEDURE

A. Experimental setup

The experiments were performed in the subsonic wind tunnel EOLE of the Pprime Institute (Poitiers, France). The flow of 40 m/s emerges from a 0.46×0.46 m^2 convergent nozzle and is guided through a 1/4 open square duct located in a $4 \times 3 \times 3$ m^3 anechoic chamber. The convergent nozzle is connected to a 1.2×0.8 m^2 manifold by two side walls. As shown in Fig. 3, the turbulences are created by a 30 mm thick panel that creates a forward-facing step. This removable panel is either a rigid instrumented flat plate [Fig. 4(a)] used for wall-pressure measurements or a 0.46×0.25 m^2 vibrating plate mounted inside a rigid frame [Fig. 4(b)]. This latter is a 3 mm thick car glass whose ρ, E, and ν' are, respectively, 2500 kg/m^3, 69 GPa, and 0.25. In addition to the flow, an acoustic source (amplified loudspeaker) is placed above the duct.

B. Flow

The classic two component particle image velocimetry (PIV) is used to measure the velocity field in the near wall plane ($z = 2$ mm) and in the symmetry plane ($y = 0$ mm). The two-dimensionality of the flow in the lateral direction improved by the side-walls has been demonstrated in a
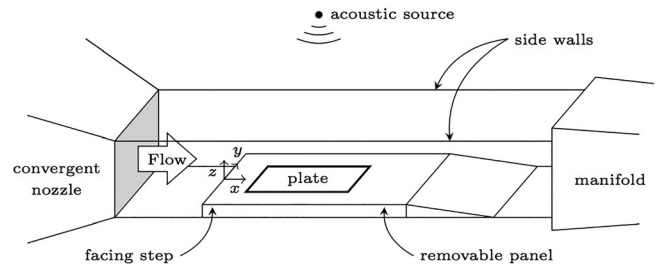

FIG. 3. Experimental setup: the wind tunnel with a flow of 40 m/s, the forward-facing step, and the additional acoustic source.
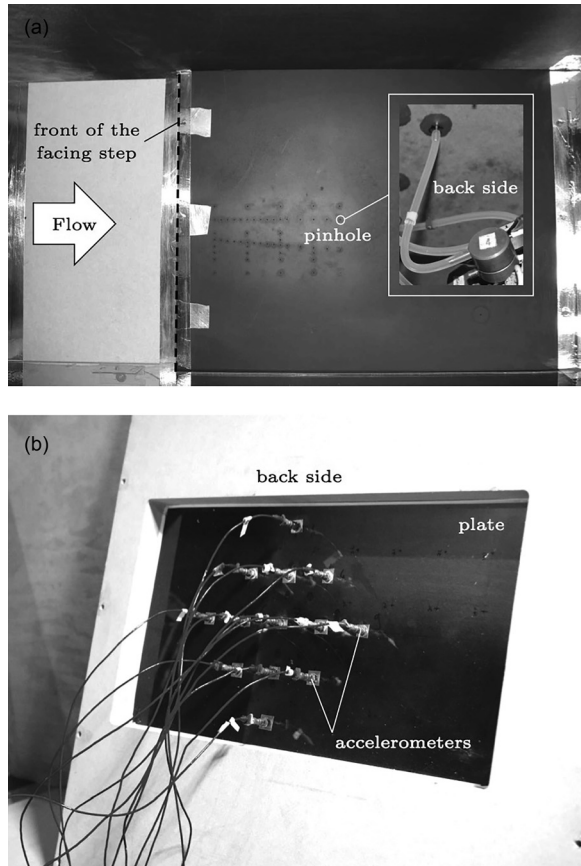
FIG. 4. The two removable panels with the two different measurement systems. (a) Top view of the step instrumented with a small insert (1.3 mm diameter) connected to a pressure sensor to the rear. (b) The vibrating plate embedded in the step and the 13-accelerometer array which measures the wall pressure at the central point of the array corresponding to the position of the pinhole shown in (a).

precedent paper[16] for the same setup and is shown in Fig. 5(a). The reattachment region is around $x = 10$ cm. In the symmetry plane [Fig. 5(b)], the streamlines reveal the mean separation bubble formed along the front of the step.

C. Wall-pressure measurements

All measurements are performed twice with two different types of sensors. The first removable panel shown in Fig. 4(a) is instrumented with a pinhole of diameter 1.3 mm connected by a small tube to a remote microphone probe at the back side of the panel. The frequency response of this system was previously characterized in a calibration tube with a reference microphone. The second removable panel, which has the same geometry as the first, is composed of the vibrating plate as shown in Fig. 4(b). An array of 13 accelerometers spaced by $\Delta = 4$ cm is placed at the rear of the plate and is used to calculate the finite difference scheme for FAT and CFAT. These methods identify the pressure at the central point of the array, which corresponds to the position of the pinhole in the first panel. Note that FAT and CFAT have a spatial resolution linked to the size of the array.[17] Even if the center of the array is not in the separation bubble region, the techniques could identify a distribution force in this area that is weak because it is smoothed and distributed in space.
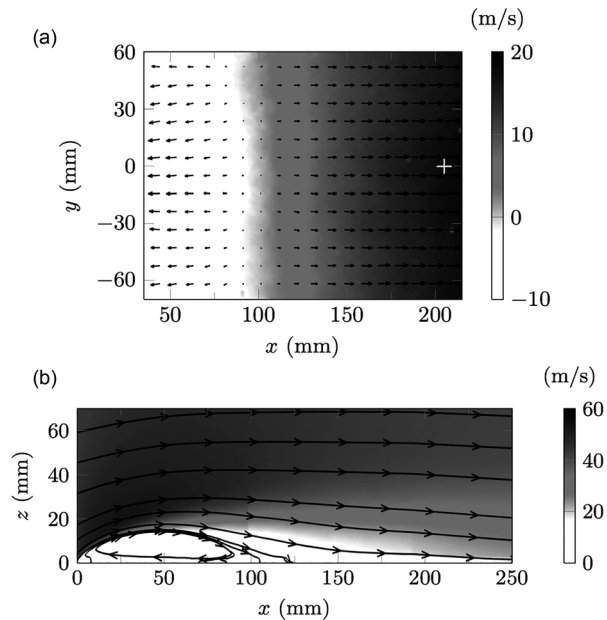

FIG. 5. Results of the PIV with a flow of 40 m/s: (a) the mean velocity along x in the near wall plane ($z = 2$ mm) where the vectors indicate the direction of the flow in longitudinal and lateral directions; (b) the mean norm velocity in the symmetry plane ($y = 0$ mm) and the streamlines. The white cross in (a) corresponds to the point where the pressure measurements are realized.

Note that the smoothing effect can be reduced by choosing a better approximation of spatial derivatives, but such a choice implies a high amplification of noise. Actually, the best chosen compromises are the use of the proposed finite differences schemes in FAT and CFAT.

D. Reference spectra of the excitations

In this study, the plate can be excited by three different excitations: the flow, a 1500 Hz sine or a white noise both generated by the loudspeaker placed above the wind tunnel. The level of the acoustic sources is set so that their spectrum is lower than that of the turbulent wall pressure for each frequency. Reference spectra of these excitations shown in Fig. 6 are successively measured by the remote pressure
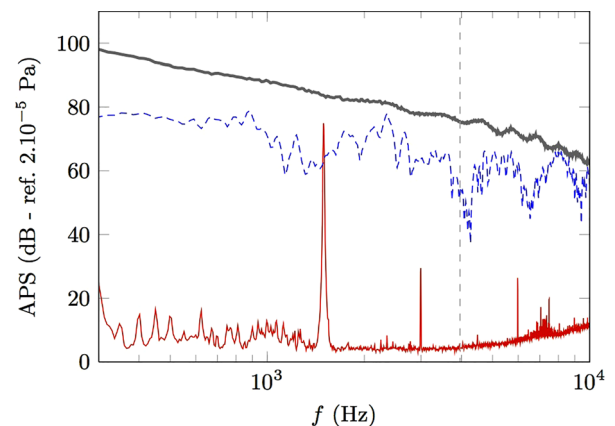

FIG. 6. (Color online) Auto power spectra (APS) of the aerodynamic (—) (flow of 40 m/s) and the acoustic excitations measured by the remote pressure sensor: 1500 Hz sine (—) and a white noise (- -). The vertical dashed line corresponds to the acoustic coincidence where $k_f = k_{ac}$.

J. Acoust. Soc. Am. **140** (3), September 2016

Lecoq *et al.* 1977

sensor of the first removable panel with a sampling frequency equals to 25.6 kHz. The averaging is performed on 359 blocks of 0.1667 s with 50% overlapping for measurements with the sine or on 959 blocks of 0.0625 s with 50% overlapping with the white noise. Note that nonnegligible harmonics appear when using the sine excitation (3 kHz, 6 kHz, etc.). These harmonics are due to the nonlinearities of the loudspeaker.

IV. EXPERIMENTAL RESULTS

A. Vibration data

Before applying the inverse problem, the vibration signals at the central point of the FAT array is presented in this section. The plate is successively excited by one of the acoustic sources, by the flow at 40 m/s and by both components. Figure 7 shows these vibration signals when the acoustic source is the 1500 Hz sine. Although the sinus is 11 dB below the turbulent flow at 1500 Hz on wall-pressure measurements (Fig. 6), the vibration of the plate excited by this acoustic component is 8 dB above the one corresponding to the excitation by the flow. When both components excite the plate, the sine is, therefore, the main source of vibration at this frequency. In addition to the harmonics 3 and 6 kHz, which were visible in the measured wall pressure (Fig. 6), the harmonics 4.5, 7.5, and 9 kHz also become nonnegligible on the vibration, because the plate is particularly sensitive to acoustic excitations for higher frequencies than its coincidence frequency.

Exactly the same observations are seen in Fig. 8, where the acoustic source is a white noise for all studied frequencies. These results highlight that the plate, in a subsonic configuration, is highly sensitive to an acoustic component with a low level and weakly sensitive to a higher aerodynamic part, which led to the same conclusion obtained in the previous study,[14] where simulations were performed for turbulent boundary layers and acoustic diffuse field excitations.

B. Spectra obtained by inverse problems

In this section, FAT and CFAT are applied to identify the spectra of the acoustic sources without flow at first, in order to validate the methods, and finally with the flow at 40 m/s.
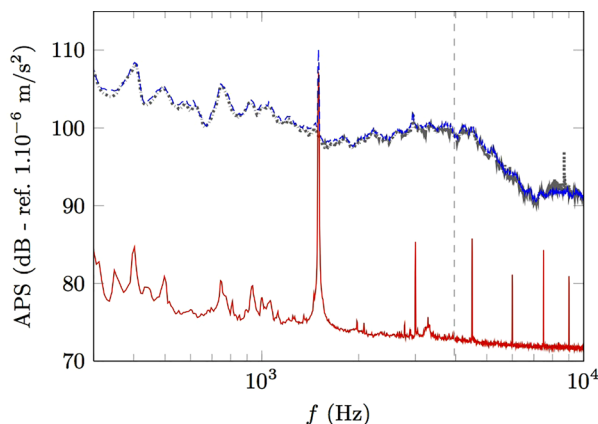
FIG. 7. (Color online) APS of the acceleration signals of the plate excited by the flow of 40 m/s (-· -), by the 1500 Hz sine (——), and by both (- -). The vertical dashed line corresponds to the acoustic coincidence.
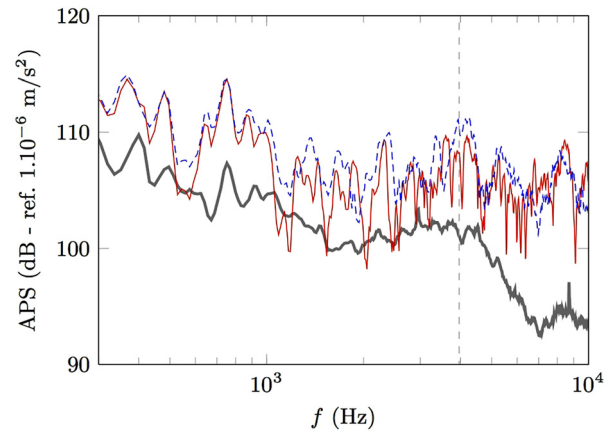
FIG. 8. (Color online) APS of the acceleration signals of the plate excited by the flow of 40 m/s (——) by a white noise (——) and by both (- -). The vertical dashed line corresponds to the acoustic coincidence.

1. Without flow

The plate is excited by the 1500 Hz sine. The spectra of the acoustic source (the same as in Fig. 6), and those of the pressures identified by FAT and CFAT are shown in Fig. 9. Both methods identify the peak at 1500 Hz with an accuracy of 1 dB and also the harmonic at 3 kHz. For the other peaks, their frequencies are higher than the coincidence frequency. Then, the excitation contains energy around the natural wavenumber k_f of the plate. This is exactly the wavenumber region where the filtering of FAT and CFAT differ drastically. This is the reason why both methods identify the peaks but give different values.

The structure is then excited by the white noise generated by the acoustic source (Fig. 10).

- In low frequencies when $\lambda_f/\Delta > 4$ ($f < 1153$ Hz), both techniques identify the white noise but they are still sensitive to noise and 10 dB differences are observable.
- For higher frequencies ($1 < f < 3$ kHz), both methods are able to measure approximately the spectrum of the acoustic
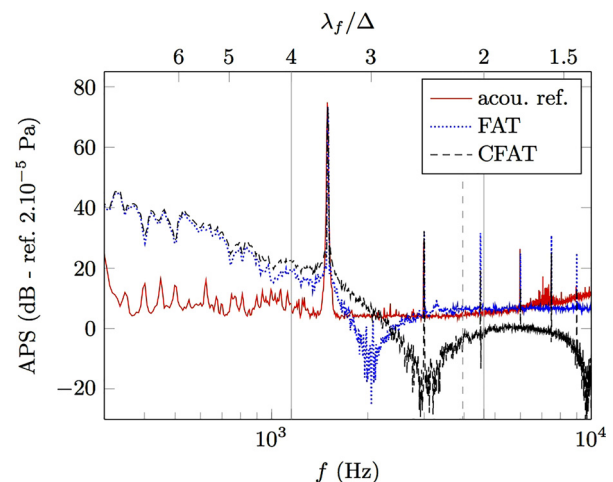
FIG. 9. (Color online) APS of the acoustic reference, the pressure identified by FAT and by CFAT for the plate excited by a sinusoidal acoustic source. Vertical solid lines indicate the frequency limits of the inverse problem, and the vertical dashed line corresponds to the acoustic coincidence.
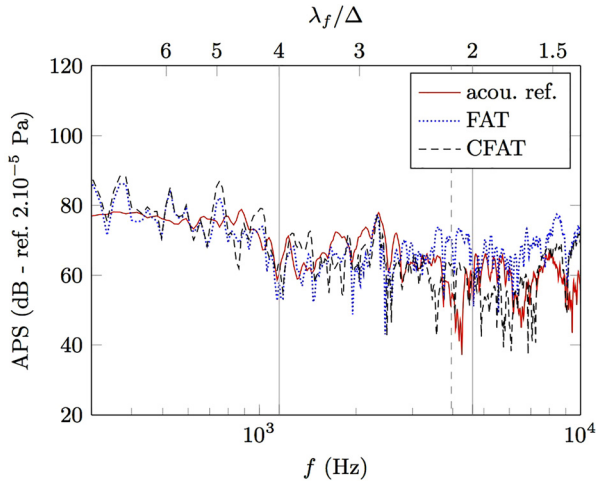
FIG. 10. (Color online) APS of the acoustic reference, the pressure identified by FAT and by CFAT for the plate excited by an acoustic white noise. Vertical solid lines indicate the frequency limits of the inverse problem, and the vertical dashed line corresponds to the acoustic coincidence.

FIG. 11. (Color online) APS of the acoustic reference (—), the pressure measured by the remote probe (—), the pressure identified by FAT (⋯), and by CFAT (- -) for the plate excited by a flow of 40 m/s and by a sinusoidal acoustic source. Vertical solid lines indicate the frequency limits of the inverse problem, and the vertical dashed line corresponds to the acoustic coincidence.

source even if some differences between the curves remain. This issue can be explained by the difference of the two measurement setups. For example, levels of acoustic radiation of panels can be different between the first panel with the pinhole and the panel comprising the vibrating plate for the FAT and CFAT measurements.

- Just before the acoustic coincidence ($f > 3$ kHz), the acoustic wavenumber k_{ac} becomes larger than the flexural wavenumber k_f. There is acoustic energy around k_f in the (k_x, k_y) plane, therefore, FAT and CFAT do not give the same results (see Fig. 2) and FAT amplifies the error at $k = k_f$, it overestimates systematically the result.

- Moreover, when $\lambda_f/\Delta < 2$ ($f > 4613$ Hz), the methods are very selective[15] and identify only the energy of the sources included in the circle of radius k_f (with their differences for $k = k_f$). That is why they do not entirely measure the acoustic excitation at these frequencies.

2. With flow

The two previous experiments are performed a second time with the flow. When the acoustic source is the sine (in Fig. 11), the peak at 1500 Hz is not visible on the spectrum measured by the remote probe since it is completely merged in the aerodynamic noise. With FAT and CFAT, this peak is detectable. This is possible because the use of vibration data enhance the SNR in the low wavenumbers for the measurement of this weak acoustic component (see Sec. IV A) and because the filtering of both methods isolates the wavenumber components below k_f. In terms of amplitude, CFAT is able to accurately measure the peak at 1500 Hz. Apart from this peak, the results obtained between 2 and 3 kHz (where both methods are valid) contain necessarily the acoustic component because this frequency range is located below the coincidence frequency 4 kHz. Note that this acoustic component can be generated by the turbulences and the acoustic radiation of the plate. The fact that FAT and CFAT give different results indicates that there exists an energy
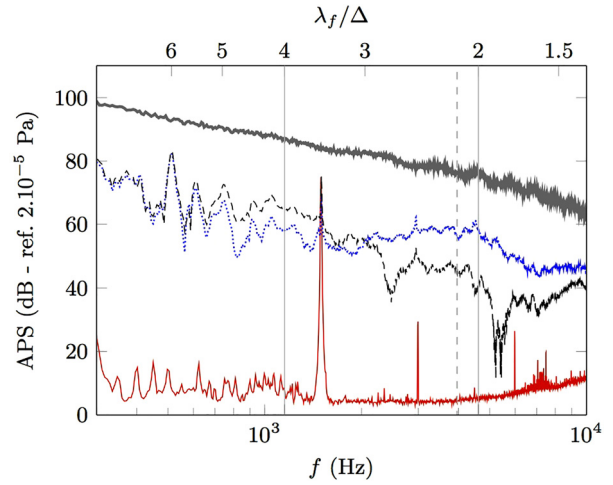
around the natural wavenumber, even if the frequencies are below the coincidence frequency. This can be explained by the fact that the pressure corresponding to the intermediate region of the wavenumber-frequency spectrum of the turbulence flow (between the acoustic and the convective regions[1]) is not negligible.

Figure 12 shows the results obtained when using the acoustic white noise excitation instead of the sine excitation. The same observation can be made, the remote sensor measures a very high pressure level, mainly due to the aerodynamic component whereas FAT and CFAT give levels close to the acoustic source in the valid frequency range of the method, even if the acoustic source is very weak compared to the aerodynamic source. Moreover, the results obtained by FAT and CFAT give similar results between 2
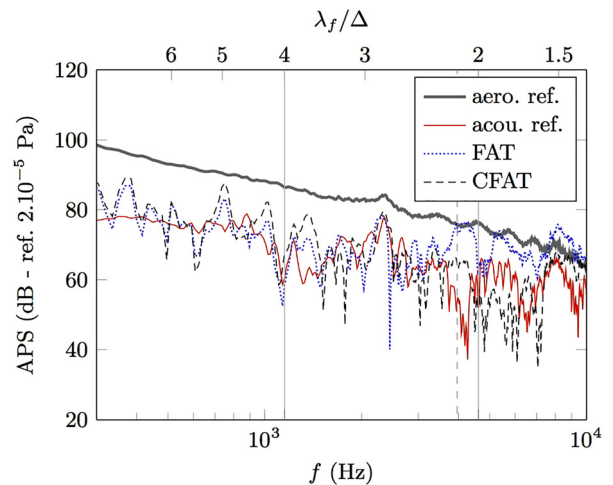

FIG. 12. (Color online) APS of the acoustic reference, the pressure measured by the remote probe, the pressure identified by FAT and by CFAT for the plate excited by a flow of 40 m/s, and by an acoustic white noise. Vertical solid lines indicate the frequency limits of the inverse problem, and the vertical dashed line corresponds to the acoustic coincidence.

J. Acoust. Soc. Am. 140 (3), September 2016

Lecoq et al.   1979

and 3 kHz. One can conclude that the information around the natural wavenumber k_f is negligible and both methods identify here only the acoustic component which is complete, because this frequency range is below the coincidence frequency (4 kHz). Around the coincidence frequency, it is clear that FAT and CFAT differ and that FAT overestimates the level.

It is particularly interesting to note that both post-processing made by FAT and CFAT allow one to analyse how the information is distributed in the wavenumber domain (in particular, around the natural wavenumber k_f), while the identification is realized in only one point.

V. CONCLUSIONS

These results confirm the conclusions previously obtained in the case of simulations,[14] especially the ability of the FAT technique to measure and isolate a weak acoustic part in a turbulent flow. Indeed, when FAT and CFAT can be designed to be valid below the coincidence frequency, the obtained results can be analyzed to see if the plate is essentially excited by the acoustic component or not. In this study, two kinds of excitations were studied. The first is a detached turbulent flow created by a forward-facing step; the second is an acoustic excitation (pure sine or white noise) whose energy is much lower. When the acoustic source is activated, it is clear that the vibration is essentially due to this source. When the turbulent flow is the only source exciting the plate, the analysis of FAT and CFAT results allows one to conclude that the acoustic component due to the turbulences and/or the plate radiation is not the only one. Indeed, the energy is present around the natural wavenumber of the plate, where the acoustic component cannot be the source, while the analysis is made below the coincidence frequency. The use of vibration data for measuring the low wavenumber part is, therefore, very convenient since they have a very good SNR for this low wavenumber. These inverse problems are simple to implement in terms of experimental setup and postprocessing; furthermore, they do not require one to know the boundary conditions because these methods are local. In terms of applications, the present study was motivated for automotive application, but they can be easily extended to other transportation industry applications, where the use of the structure as a sensor gives an interesting nonintrusive wall pressure measurement technique. It will also be interesting to study its use for supersonic or hypersonic applications (aircraft, aerospace industries), where the relationship between the acoustic and the aerodynamic components are very different. For more complex structures, an adaptation of FAT to structures modeled by finite element method exists,[18,19] but the wavenumber filtering notion makes no sense here; the benefit of the FAT/CFAT analysis should be considered in a different manner.

[1] W. K. Blake, *Mechanics of Flow-Induced Sound and Vibration, Vols. 1 and 2* (Academic, New York, 1986).

[2] M. K. Bull, "Wall-pressure fluctuations beneath turbulent boundary layers: Some reflections on forty years of research," J. Sound Vib. **190**, 299–315 (1996).

[3] M. S. Howe, "Surface pressures and sound produced by turbulent flow over smooth and rough walls," J. Acoust. Soc. Am. **90**, 1041–1047 (1991).

[4] G. M. Corcos, "Resolution of pressure in turbulence," J. Acoust. Soc. Am. **35**, 192–199 (1963).

[5] D. M. Chase, "Modeling the wavevector-frequency spectrum of turbulent boundary layer wall pressure," J. Sound Vib. **70**, 29–67 (1980).

[6] D. M. Chase, "The character of the turbulent wall pressure spectrum at subconvective wavenumbers and a suggested comprehensive model," J. Sound Vib. **112**, 125–147 (1987).

[7] G. Maidanik, "Flush-mounted pressure transducer systems as spatial and spectral filters," J. Acoust. Soc. Am. **42**, 1017–1024 (1967).

[8] G. Maidanik and D. W. Jorgensen, "Boundary wave-vector filters for the study of the pressure field in a turbulent boundary layer," J. Acoust. Soc. Am. **42**, 494–501 (1967).

[9] W. K. Blake and D. M. Chase, "Wavenumber-frequency spectra of turbulent boundary layer pressure measured by microphone arrays," J. Acoust. Soc. Am. **47**, 92 (1970).

[10] C. H. Sherman, S. H. Ko, and B. G. Buehler, "Measurement of the turbulent boundary layer wave-vector spectrum," J. Acoust. Soc. Am. **88**, 386–390 (1990).

[11] B. Arguillat, D. Ricot, C. Bailly, and G. Robert, "Measured wavenumber: Frequency spectrum associated with acoustic and aerodynamic wall pressure fluctuations," J. Acoust. Soc. Am. **128**, 1647–1655 (2010).

[12] N. C. Martin and P. Leehey, "Low wavenumber wall pressure measurements using a rectangular membrane as a spatial filter," J. Sound Vib. **52**, 95–120 (1977).

[13] C. Pézerat and J.-L. Guyader, "Force analysis technique: Reconstruction of force distribution on plates," Acta Acust. Acust. **86**, 322–332 (2000).

[14] D. Lecoq, C. Pézerat, J.-H. Thomas, and B. Wenping, "Extraction of the acoustic component of a turbulent flow exciting a plate by inverting the vibration problem," J. Sound Vib. **333**, 2505–2519 (2014).

[15] Q. Leclère and C. Pézerat, "Vibration source identification using corrected finite difference schemes," J. Sound Vib. **331**, 1366–1377 (2012).

[16] R. Béssis, L.-E. Brizzi, and Y. Gervais, "Experimental correlations between aerodynamics, wall-pressure fluctuations, and noise transmission through a window downstream of a step in a flow," Int. J. Aerodyn. **4**(1-2), 87–107 (2014).

[17] C. Pézerat and J.-L. Guyader, "Two inverse methods for localization of external sources exciting a beam," Acta Acust. **3**(1), 1–10 (1995).

[18] C. Renzi, C. Pezerat, and J.-L. Guyader, "Vibratory source identification by using the finite element model of a subdomain of a flexural beam," J. Sound Vib. **332**, 545–562 (2013).

[19] C. Renzi, C. Pézerat, and J.-L. Guyader, "Local force identification on flexural plates using reduced finite element models," Comput. Struct. **144**, 75–91 (2014).